

FEDSM-ICNMM2010-30688

HIGH ORDER SLIP AND THERMAL CREEP EFFECTS IN MICRO CHANNEL NATURAL CONVECTION

Hamid Niazmand*

Department of Mechanical engineering
Ferdowsi University of Mashhad
Mashhad, IRAN

Behnam Rahimi

Department of Mechanical engineering
Ferdowsi University of Mashhad
Mashhad, IRAN
Behnam.rahimi@Hotmail.com

ABSTRACT

Developing natural convection gaseous flows in an open-ended parallel plate vertical microchannel with isothermal wall conditions are numerically investigated to analyze the rarefaction effects on heat transfer and flow characteristics in slip flow regime. The Navier-Stokes and energy equations are solve by a control volume technique subject to higher-order temperature jump and velocity slip conditions including thermal creep effects. The flow and thermal fields in the entrance and fully developed regions along with the axial variations of velocity slip, temperature jump, and heat transfer rates are examined in detail. It is found that rarefaction effects significantly influence the flow and thermal fields such that mass flow and heat transfer rates are increased considerably as compared to the continuum regime. Furthermore, thermal creep contribution to the velocity slip is found to be dominant close to the channel inlet and vanishes in the fully developed region, while velocity slip approaches a finite value there. Both Mass flow rate and thermal entrance length increase with increasing Knudsen number in slip flow regime.

INTRODUCTION

In recent years, fluid flow and heat transfer in microscale devices have become a popular research topic due to the rapid growth of practical applications in micrototal analysis systems and micro electro mechanical systems (MEMS), Such as micro-heat exchangers [1], microactuators and microreactors [2], to name a few. Many of these devices are associated with gas flow through micron sized channels, known as microchannels.

It has been reported that the continuum hypotheses may not be valid for microchannel flows. A dimensionless parameter that indicates the extent of deviation from continuum is called Knudsen number defined as the ratio of mean free path to the characteristic length of the system (see Fig. 1) [3]. Classical

Navier–Stokes equations with no-slip wall boundary conditions based on the continuum model are only accurate for small values of Knudsen number ($Kn < 0.001$). Flow with Knudsen number ranging from 0.001 to 0.1 is called slip flow regime, where some degrees of rarefaction effects are present. It is well established that for slip flow regime Navier–Stokes equations can still be used with modified boundary conditions that are velocity slip and temperature jump conditions [4-6]. However, when Knudsen number exceeds 0.1, the so called transitional regime, the continuum hypothesis gradually breaks down, and for Knudsen numbers greater than 10, flow regime is known as free molecular regime due to negligible collision among molecules.

The thermal creep phenomenon is a rarefaction effect, which is related to the streamwise temperature gradient of the fluid. There is a possibility to generate a flow due to tangential temperature gradients along the micro channel walls, which move the fluid in the direction of increasing temperature. In gaseous microflows even with constant wall temperature, due to temperature jump condition, streamwise temperature gradients exist in the first layer of gas adjacent to the walls. Therefore, in such flows the momentum and energy equations are coupled through thermal creep effects.

Natural convection has been applied to many engineering fields, such as microelectrochemical cell transport, microheat exchanging and microchip cooling, because of its reliability, low manufacturing and maintaining costs [7]. Natural convection is also an area of interest for enhancement of heat and mass transfers in bio-chemical systems and in micro-fuel cell devices [8].

In contrast to the forced convection that has received proper attention in literature, very limited information is available with regard to the micro scale natural convection. One of the early studies is presented by Chen and Weng in 2005 [9].

* Author of correspondence

NOMENCLATURE

b	high-order slip coefficient
c_p	specific heat at constant pressure
D	width of channel
g	gravitational acceleration
H	height of channel
k	thermal conductivity
Kn	Knudsen number ($\frac{\lambda}{D}$)
Nu	local Nusselt number
p	pressure
Ra	Rayleigh number based on ambient properties
T	temperature
u, v	velocity components in x, y directions
U	dimensionless velocity component in x direction
V	dimensionless velocity component in y direction ($\frac{v * Ra}{v_c}$)
x, y	rectangular coordinate system
X, Y	dimensionless rectangular coordinate system

Greek letters

β	thermal expansion coefficient
γ	specific heat ratio
λ	molecular mean free path
θ	dimensionless temperature
μ	shear viscosity
ρ	density
σ_t	thermal accommodation coefficient
σ_v	tangential momentum accommodation coefficient

Subscripts

ave	average value in the y-direction
c	characteristic value
g	gas value near the wall surface
n	no-slip values
0	ambient values
s	wall-slip values
w	wall values

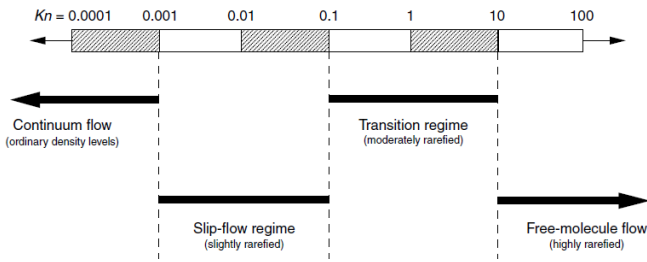


Figure 1. FLOW CHARACTERIZATION ACCORDING TO THE KNUDSEN NUMBER.

They have considered fully developed natural convection in a vertical parallel-plate microchannel analytically and shown that rarefaction effects enhance flow rate, while reducing the heat transfer rate. Implicit finite difference simulation of the developing natural convective gas microflow was presented by Haddad et al. [10]. Their case study was an isothermally heated microchannel filled with porous media. Biswal et al. [11] investigated the flow and heat transfer characteristics in the developing region of an isothermal microchannel using the semi-implicit method for pressure linked equations (SIMPLE). They also showed micro scale effects result in heat transfer enhancements. Chen and Weng [12] used a marching implicit procedure for modeling developing natural convection in micro channels to show the importance of thermal creep and high-order slip/jump conditions. Chakraborty et al. [13] executed boundary layer integral analysis to investigate the heat transfer characteristics of natural convective gas microflows in symmetrically heated vertical channels. Avci and Aydin [14, 15] studied mixed convective gas microflow in vertical channel for both constant wall temperature and heat flux conditions. Chen

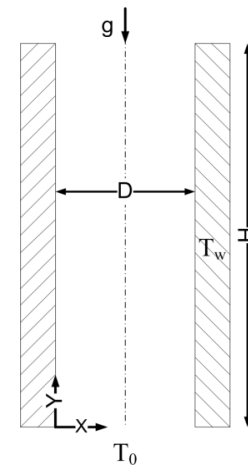


Figure 2. FLOW GEOMETRY AND THE COORDINATES SYSTEM.

and Weng [16] emphasized the importance of thermal creep in natural convective gas microflow with constant wall heat fluxes using analytical solution for fully developed region. Later, Weng and Chen [17] investigated natural convective gas microflow using analytical solution of fully developed region in an open-ended vertical annular isothermally heated microchannel. The aim of the present research is to execute a comprehensive computational study on natural convective gas micro flow in an open-ended vertical micro channel. A numerical solution for developing and fully developed regions considering temperature jump and velocity slip with thermal creep boundary conditions is presented. The second order slip/jump conditions with thermal creep are considered without simplifications that have considered in previous studies [12, 13]. The rarefaction and thermal creep effects on heat and mass

flow rates are examined in detail, while comparing with macro scale solutions.

PROBLEM FORMULATIONS

Consider a vertical parallel plate microchannel and Cartesian coordinates x and y , as shown in Fig. 2. Channel height (H) is chosen much larger than its width (D) to ensure the fully developed flow conditions at the channel exit. Both ends of the channel are open to the ambient with density ρ_0 and temperature T_0 . Vertical plates are kept at uniform temperature of T_w , which is larger than the ambient temperature. The effects of compressibility and viscous dissipations are neglected due to low speed flows associated with microchannel. Under the Boussinesq approximation, the governing equations for two dimensional, steady, and laminar flow are the following:

Continuity

$$\frac{\partial u}{\partial x} + \frac{\partial v}{\partial y} = 0 \quad (1)$$

X-momentum

$$\rho \left(u \frac{\partial u}{\partial x} + v \frac{\partial u}{\partial y} \right) = - \frac{\partial p}{\partial x} + \frac{\partial}{\partial x} \left(\mu \frac{\partial u}{\partial x} \right) + \frac{\partial}{\partial y} \left(\mu \frac{\partial u}{\partial y} \right) \quad (2)$$

Y-momentum

$$\rho \left(u \frac{\partial v}{\partial x} + v \frac{\partial v}{\partial y} \right) = - \frac{\partial p}{\partial y} + \frac{\partial}{\partial x} \left(\mu \frac{\partial v}{\partial x} \right) + \frac{\partial}{\partial y} \left(\mu \frac{\partial v}{\partial y} \right) + \rho g \beta (T - T_0) \quad (3)$$

Energy

$$\left(u \frac{\partial(\rho c_p T)}{\partial x} + v \frac{\partial(\rho c_p T)}{\partial y} \right) = \frac{\partial}{\partial x} \left(k \frac{\partial T}{\partial x} \right) + \frac{\partial}{\partial y} \left(k \frac{\partial T}{\partial y} \right) \quad (4)$$

where β is volumetric thermal expansion coefficient, μ is the dynamic viscosity, c_p is the specific heat at constant pressure and k is thermal conductivity. Based on the gas kinetic theory, the Maxwell slip model relates the slip velocity to the local velocity gradient at the wall as[18]:

$$v_s = \frac{2 - \sigma_v}{\sigma_v} KnD \left(\frac{\partial v}{\partial x} \right)_g + \frac{3}{2\pi} \frac{\gamma - 1}{\gamma} \frac{c_p \rho_0}{\mu_0} (\lambda)^2 \left(\frac{\partial T}{\partial y} \right)_g \quad (5)$$

The second term in slip condition is associated with thermal creep. For molecules that are not thermally accommodated with the wall, there is a temperature discontinuity and kinetic theory expression for temperature jump is [19]:

$$T_s = T_w + \frac{2 - \sigma_t}{\sigma_t} \frac{2\gamma}{\gamma + 1} KnD \left(\frac{1}{Pr} \frac{\partial T}{\partial x} \right)_g \quad (6)$$

Here γ is the specific heat ratio. σ_v and σ_t are the tangential momentum and energy accommodation coefficients, which are determined experimentally. However, for most engineering applications they are around one and therefore, are taken as one in the present study [12]. These slip/jump boundary conditions with thermal creep are accurate up to first-order terms in Kn. Beskok and Karniadakis [6] proposed a formulation that developed slip/jump boundary conditions accurate up to the second order terms in Knudsen number. They introduced an empirical parameter named high-order slip coefficient as follows:

$$b = \frac{1}{2} D \frac{\frac{\partial^2 v_n}{\partial x^2}}{\frac{\partial v_n}{\partial x}} \quad (7)$$

where the subscript n refers to the corresponding no-slip solution. It was proposed that a second order accurate slip/jump formula can be obtained by replacing the molecular mean free path $\lambda = KnD$ in Eqs. 5 and 6 by:

$$\frac{D\lambda}{D - b\lambda} \quad (8)$$

As for boundary conditions, $u = 0$, $v = v_{avg}$ and $T = T_0$ are assumed for the inlet boundary conditions. It should be noted that v_{avg} is updated according to the exit mass flow rate at each iteration. For all flow variables zero gradients at outlet are applied. At walls slip velocity and temperature jump are considered. Governing equations are solved using a finite volume approach. The convective terms are discretized using the power-law scheme, while for diffusive terms the central difference is employed. Coupling between the velocity and pressure is made with SIMPLE algorithm[19]. The resultant system of discretized linear algebraic equations is solved with an alternating direction implicit scheme (ADI).

Extensive computations have been performed to identify the number of grid points that produces reasonably grid independent results. It was found that the solution is very sensitive to the number of grid points in the axial direction. In fact the grids must be dense enough around the microchannel inlet to properly resolve the dramatic variations in the axial velocity profiles. Therefore, the minimum grid points of 50x1850 are used in the cross sectional and axial directions, respectively. The grid points are clustered toward the inlet and the walls with the expansion ratio of 1.01 and 1.03 respectively.

RESULTS AND DISCUSSION

First the numerical scheme has been validated by

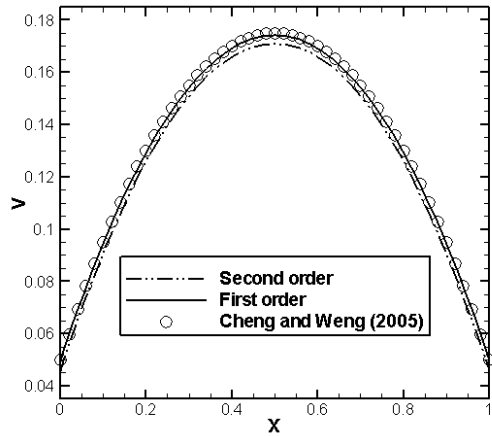


Figure 3. COMPARISON OF THE FULLY DEVELOPED NUMERICAL VELOCITY PROFILES WITH THE ANALYTICAL SOLUTION OF [9] AT $Kn=0.1$.

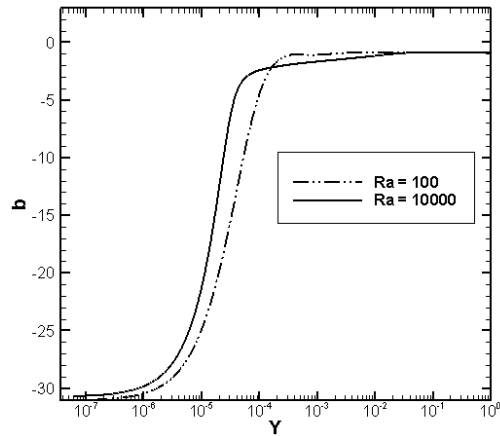


Figure 4. AXIAL VARIATIONS OF THE HIGH-ORDER SLIP COEFFICIENT, $b(y)$.

comparing the fully developed velocity profile with the analytical solution of Chen and Weng[9] as shown in Fig. 3. In this figure the fully developed velocity profiles for $Kn = 0.1$ are plotted for both first and second order accurate velocity slip and temperature jump conditions. The length and velocity in Fig. 3 are nondimensionalized as $X = \frac{x}{D}$ and $V = \frac{v}{v_c}$ where characteristics velocity, v_c , is defined as:

$$v_c = \frac{\rho g \beta (T_w - T_0) D^2}{\mu} \quad (9)$$

Clearly, the numerical velocity profiles, especially the first order accurate profile, are in good agreements with the first order analytical solution of Chen and Weng[9].

As mentioned earlier, the second order approximations for velocity slip and temperature jump are based on the empirical parameter expressed by Eq. (7). The axial variations of this parameter, $b(y)$, are plotted in Fig. 4 for two different Rayleigh

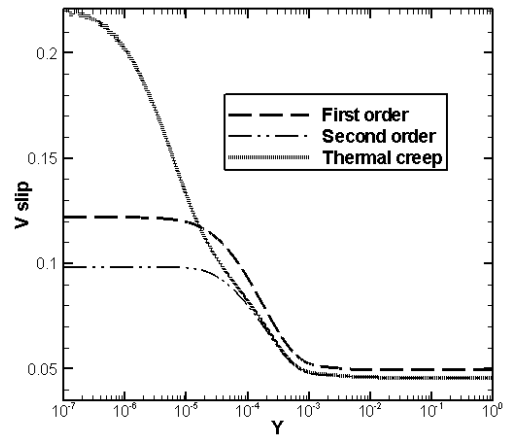


Figure 5. COMPARISON OF THE AXIAL VARIATIONS OF THE FIRST AND SECOND ORDER VELOCITY SLIP.

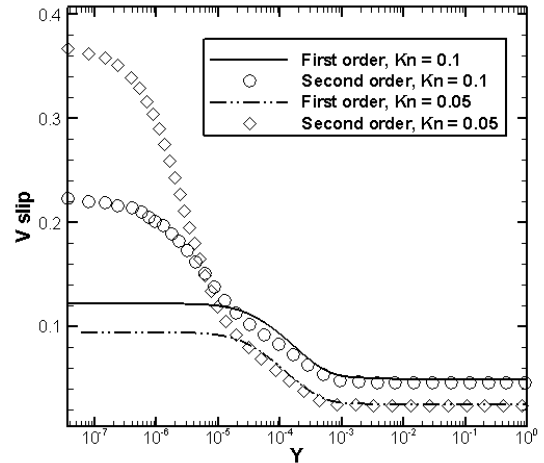


Figure 6. RARFACTIONS EFFECTS ON THE AXIAL VARIATIONS OF THE VELOCITY SLIP.

numbers defined as $Ra = \frac{\rho_0^2 c_{p0} g \beta_0 D^3 (T_w - T_0)}{\mu_0 k_0}$. The axial direction, y , in all of the following figures is normalized with respect to the channel height $Y = y/H$. It is observed that an initial abrupt rise in b is followed by a gradual increase to the asymptotic value of -1 in the fully developed region[6]. Clearly, the higher order effects are most important in the early sections of the microchannel, where the flow is developing from a uniform inlet profile to the fully developed parabola and thus large normal velocity gradients exist. Figure also shows that the high order parameter is slightly influenced by the Rayleigh number. The second order effects on velocity slip can be seen in Fig. 5, where the first and second order axial variations of velocity slip are compared. The contribution of the thermal creep is shown separately for the second order accurate case only. It is observed that second order effects reduce the velocity slip especially in the developing region of the channel. However, thermal creep effects which are dominant in this region increase the velocity slip considerably. In the fully developed region, the velocity slip approaches a constant value

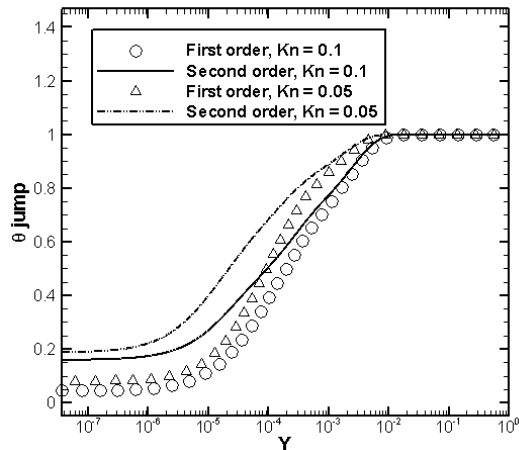


Figure 7. RARFACTION EFFECTS ON THE AXIAL VARIATIONS OF THE TEMPERATURE JUMP.

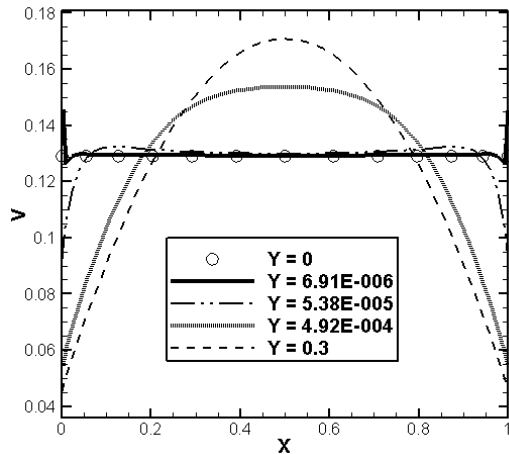


Figure 8. STREAMWISE VELOCITY PROFILES AT DIFFERENT AXIAL LOCATIONS FOR Kn=0.1.

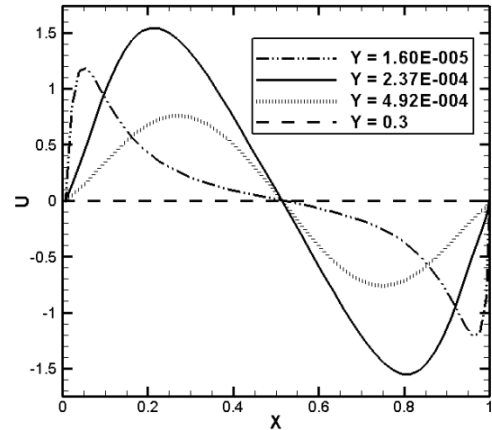


Figure 9. CROSS-FLOW VELOCITY PROFILES AT DIFFERENT AXIAL LOCATIONS FOR Kn=0.1.

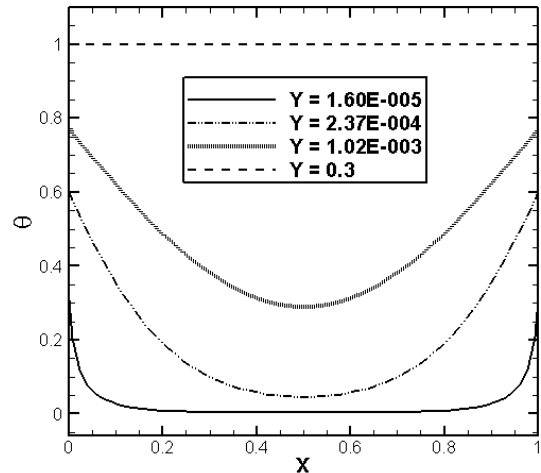


Figure 10. TEMPERATURE DISTRIBUTION AT DIFFERENT AXIAL LOCATIONS FOR Kn=0.1.

since the velocity profiles remain constant and the normal velocity gradients become invariant. It must be emphasized that the thermal creep contribution to the velocity slip vanishes in the fully develop region where the axial temperature gradients are basically zero.

In Fig. 6 the rarefaction effects on the axial variations of the slip velocity are presented. First order slip velocity variations are also included for comparison, however, thermal creep effects are only considered in the second order slip cases.

As indicated by equation 5, normal velocity gradient contribution to the velocity slip is directly related to Kn, and therefore, increases at higher Knudsen numbers as is the case for the first order velocity slip variation along the channel, where thermal creep is neglected. However, as can be seen for the second order velocity slip, where thermal creep effects are considered velocity slip is larger at lower Kn just close to the inlet. The fact can be explained by Fig. 7, where rarefaction effects on axial variations of the temperature jump according to Eq. (6) are shown. The non-dimensional temperature

jump, $\theta_s = \frac{T_s - T_0}{T_w - T_0}$, is considerable close to the inlet, where uniform temperature inflow is exposed to the heated wall leading to large normal temperature gradients. It is clear that close to the entrance the axial gradients of θ_s , which are directly reflected in the velocity slip, are larger at lower Knudsen numbers. Therefore, at lower Kn the normal velocity component to the velocity slip decreases, while the thermal creep effect increases. Since thermal creep contribution to the velocity slip is dominant close to the inlet, it compensates for the reduction in normal velocity component and the outcome is an increase in the velocity slip at lower Kn just very close to the inlet. From Figs. 6 and 7, it is also notice that the second order effects are basically negligible in the fully developed region.

As for temperature jump in Fig. 7, the second order effects also decrease the temperature differences between the wall and the first layer of gas adjacent to the wall. As flow gradually heats up along the channel it approaches the wall temperature and therefore temperature jump vanishes in the

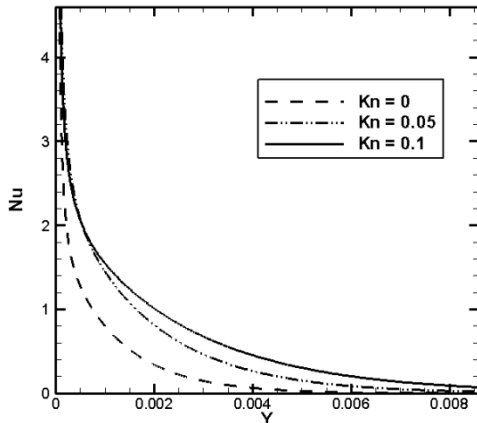


Figure 11. RAREFACTION EFFECTSON THE AXIAL VARIATIONS OF THE HEAT TRANSFER RATES.

fully developed region. This is in contrast to the velocity slip, which is finite and constant in the fully developed region.

Now that the axial variations of the velocity slip and temperature jump are discussed, the developments of profiles can be examined. Figures 8 and 9 present the streamwise and cross-flow velocity profiles normalized by the characteristic velocity defined by Eq. (9). However, the cross-flow profiles are also multiplied by the associated flow Rayleigh number for more clarifications. Second order velocity slip is considered including thermal creep for $Kn = 0.1$. It is observed from Fig. 8 that the uniform inlet velocity profile transforms into the fully developed profile after passing through considerable changes. Very close to the inlet, the velocity slip due to the thermal creep effects and large normal velocity gradients is so strong that the axial velocity of the gas layer adjacent to the wall is even higher than the inlet velocity. However, this effect is limited to the immediate vicinity of the wall, which is followed by a thin layer of the fluid with slightly lower velocity than the inlet velocity to satisfy the conservation of mass. Velocity slip at wall drops dramatically right after the inlet, as discussed with respect to the Fig. 6, yet, velocity profile is still flat with small overshoots close to the wall at axial location of $Y=5.38E-5$. The axial velocity profile becomes fully developed as thermal creep effect vanishes and the velocity slip reaches its constant fully developed value. Cross flow field forms close to the entrance due to the uniform inlet velocity profile and dragging effect of the wall as shown in Fig. 9. Even with large velocity slip at wall the fluid slows down by the wall leading to regions of high pressure at wall close to the inlet. These localized high pressure zones at the inlet walls push the fluid toward the core which generates the cross flow, and also push the fluid in the axial direction which forms the overshoots in the axial profiles observed in Fig. 8 close to the inlet. Cross-flow is strong close to the inlet and smears out toward the fully developed region, where cross sectional pressure variation vanishes.

In Fig. 10 the developments of temperature profiles along the microchannel are presented for the same flow conditions as those in Fig. 8. Temperature profiles indicate large temperature

jumps close to the inlet, which disappear as the fluid approaches the wall temperature and normal and axial temperature gradients vanish. In contrast to the no slip conditions, where the temperature difference between the fluid at the wall and the core region reduces continuously, this temperature difference for microchannels in slip flow regime increases first due to the reduction in temperature jump and then reduces until the fluid reaches the wall temperature.

The rarefaction effects on the variations of the Nusselt number along the microchannel are presented in Fig. 11. Clearly, rarefaction effects increase the heat transfer rate, yet, this is not a trivial matter since there are opposing effects involved. Considering the nature of the temperature jump that reduces the normal temperature gradients, it basically acts as a thermal contact resistance which reduces the heat transfer rates. On the other hand, velocity slip at the wall increases the mass flow rate and also the entrance length as is clear from Fig. 11, which both factors increase the heat transfer rate. Apparently, the enhancing factors outweigh the contact resistance effect and for the present problem the averaged Nusselt number increases about 50% for $Kn=0.1$, and about 25% for $Kn=0.05$ as compared to that of the no slip conditions.

CONCLUSIONS

A numerical analysis on the developing and developed natural convective gas flows through a symmetrically heated vertical microchannel, under the condition of large channel aspect ratio, has been performed. The governing equations subject to the second order slip/jump boundary conditions including thermal creeps are solved numerically, using a control volume method. The validation was established through comparison of numerical velocity profiles with their analytical counterparts. The results were presented for both first order and second order slip/jump approximations including thermal creep effects. The major observation from the present study can be summed up as follows:

- (i) Velocity slip is slightly over predicted by the first order slip/jump approximation as compared to the second order approximation, especially close to the microchannel inlet. This is in contrast to the temperature of first layer of gas, which is under predicted by the first order slip/jump approximation.
- (ii) Thermal creep contribution to the velocity slip is dominant close to the channel inlet and vanishes in the fully developed region.
- (iii) Temperature jump is basically zero in the fully developed region, while velocity slip has a finite value.
- (iv) Mass flow rate and thermal entrance length are both enhanced with increasing Knudsen number in slip flow regime.
- (v) Rarefaction effects increase the heat transfer rates as compared to the continuum limit no slip condition.

REFERENCES

- [1] Wu, P., Little, WA., 1984. "Measurement of the heat

- transfer characteristics of gas flow in fine channel heat exchangers used for microminiature refrigerators”. *Cryogenics*, 24, pp. 415-420.
- [2] Kobayashi, J., Mori, Y., Okamoto, K., Akiyama, R., Ueno, M., Kitamori, T., Kobayashi, S., 2004. “A Microfluidic Device for Conducting Gas-Liquid-Solid Hydrogenation Reactions”. *Science*, 304, pp. 1305-1308.
- [3] Gad-El-Hak, M., 2001. *The MEMS Handbook*, CRC Press.
- [4] Karniadakis, GE., Beskok, A., 2002. *Microflows: Fundamentals and Simulation*, Springer-Verlag, New York.
- [5] Beskok, A., Karniadakis, GE., Trimmer, W., 1996. “Rarefaction and Compressibility Effects in gas Microflows”. *J fluid Eng*, 118, pp.448-456.
- [6] Beskok, A., Karniadakis, GE., 1999. “A model for flows in channels, pipes, and ducts at micro and nano scales”. *Microscale Thermophysical Engineering*, 3, pp. 43-77.
- [7] Weng, HC., Chen, CK., 2008. “Variable physical properties in natural convective gas microflow”. *Journal of Heat Transfer*, 130.
- [8] Banerjee, S., Mukhopadhyay, A., Sen, S., Ganguly, R., 2008. “Natural convection in a bi-heater configuration of passive electronic cooling”. *International Journal of Thermal Sciences*, 47, pp. 1516-1527.
- [9] Chen, CK., Weng, HC., 2005. “Natural convection in a vertical microchannel”. *Journal of Heat Transfer*, 127, pp. 1053-1056.
- [10] Haddad, O M., Abuzaid, M M., Al-Nimr, M A., 2005, “Developing Free-Convection Gas Flow in a Vertical Open-Ended Microchannel Filled with Porous Media”. *Numerical Heat Transfer Part A: Applications*, 48, pp. 693-710.
- [11] Biswal, L., Som, SK., Chakraborty, S., 2007. “Effects of entrance region transport processes on free convection slip flow in vertical microchannels with isothermally heated walls”. *International Journal of Heat and Mass Transfer*, 50, pp. 1248-1254.
- [12] Chen, CK., Weng, HC., 2006. “Developing natural convection with thermal creep in a vertical microchannel”. *Journal of Physics D: Applied Physics*, 39, pp. 3107-3118.
- [13] Chakraborty, S., Som, SK., Rahul, 2008. “A boundary layer analysis for entrance region heat transfer in vertical microchannels within the slip flow regime”. *International Journal of Heat and Mass Transfer*, 51, pp. 3245-3250.
- [14] Avci, M., Aydin, O., 2007. “Mixed convection in a vertical parallel plate microchannel with asymmetric wall heat fluxes”. *Journal of Heat Transfer*, 129, pp. 1091-1095.
- [15] Avci, M., Aydin, O., 2007. “Mixed convection in a vertical parallel plate microchannel”. *Journal of Heat Transfer*, 129, pp. 162-166.
- [16] Weng, HC., Chen, CK., 2008. “On the importance of thermal creep in natural convective gas microflow with wall heat fluxes”. *Journal of Physics D: Applied Physics*, 41.
- [17] Weng, HC., Chen, CK., 2009. “Drag reduction and heat transfer enhancement over a heated wall of a vertical annular microchannel”. *International Journal of Heat and Mass Transfer*, 52, pp. 1075-1079.
- [18] Maxwell, JC., 1879. “On Stress in Rarefied Gases From Inequalities of Temperature”. *Philos Trans R Soc London*, 170, pp. 231-256.
- [19] Kennard, E., 1938. *Kinetic Theory of Gases*. McGraw-Hill Book Co, New York.
- [20] Patankar, SV., 1980. *Numerical Heat Transfer and Fluid Flow*. McGraw-Hill, New York.